HHS Public Access

Author manuscript

Adv Healthc Mater. Author manuscript; available in PMC 2016 December 30.

Published in final edited form as:

Adv Healthc Mater. 2015 December 30; 4(18): 2797–2801. doi:10.1002/adhm.201500491.

Carbohydrate-Conjugated Hollow Oblate Mesoporous Silica Nanoparticles as Nanoantibiotics to Target Mycobacteria

Dr. Nanjing Hao, **Xuan Chen**, **Dr. Seaho Jeon**, and **Prof. Dr. Mingdi Yan**

Department of Chemistry, University of Massachusetts, Lowell, MA 01854, USA. Fax: +1-978-934-3013; Tel: +1-978-934-3647

Mingdi Yan: mingdi_yan@uml.edu

Abstract

Engineering nanomaterials with enhanced antibacterial activities remains a critical and practical challenge. Hollow oblate mesoporous silica nanoparticles (HOMSNs) are synthesized by a simple protocol of ammonia hydrothermal treatment of oblate mesoporous silica nanoparticles prepared using dibenzyl ether as a co-solvent. When conjugate with trehalose as the targeting ligand, the antibiotic-encapsulated HOMSNs exhibit high binding affinity and antibacterial efficacy towards mycobacteria.

Keywords

targeting; antimicrobial; trehalose; nanoantibiotic; mesoporous silica nanoparticle

The increased risk of drug resistance associated with the over-use of antibiotics is becoming a major concern for global public health, which calls for effective antibiotic alternatives.[1] Mesoporous silica nanoparticles (MSNs) have recently attracted significant interest in cancer therapy, tissue engineering, bioseparation, protein transportation, gene transfection, biosensor, catalysis, and bioimaging.[2] MSNs as drug carriers have unique advantages including exceptionally high surface area, controlled pore size and surface chemistry which allow the loading of diverse molecular cargos at levels exceeding those of other delivery systems. Both polar and non-polar drugs have been loaded singly or in combination at high concentrations. However, MSNs are rarely used in targeted drug delivery for bacteria. This situation may be partly due to the lack of targeting strategies for nanoparticles to bind and gain entry into bacteria.[3] Therefore, developing mesoporous silica-based nanoantibiotics that could specifically target bacteria of interest is the essential first step for the efficient delivery of antimicrobial agents.

Non-spherical nanoparticles have shown, both theoretically and experimentally, enhanced cell binding efficiency, cell uptake kinetics, drug loading capacity, sustained release profile and cell functions in comparison to their spherical counterpart.[4] Hollow mesoporous silica

Correspondence to: Mingdi Yan, mingdi_yan@uml.edu.

Supporting Information

Supporting Information is available from the Wiley Online Library or from the author.

nanoparticles having large interior cavity and permeable mesoporous shell is another unique type of nanomaterials that have outstanding properties including low density, high surface-to-volume ratio, and high mechanical and thermal stability.[5] Therefore, non-spherical hollow mesoporous silica nanoparticles may combine the properties of non-spherical nanoparticles with those of hollow mesoporous silica nanoparticles to afford unique and superb properties suited for antimicrobial applications.

Herein, we report a simple protocol for the synthesis of hollow oblate mesoporous silica nanoparticles (HOMSNs) by subjecting oblate mesoporous silica nanoparticles (OMSNs) to ammonia hydrothermal treatment. The ability of these new HOMSNs as drug delivery system was tested for their antimicrobial activities against mycobacteria. Some mycobacteria, including TB-causing *Mycobacterium tuberculosis*, are serious intracellular pathogens that can invade and survive within host cells, and are a major health threat worldwide.[6] Trehalose, a non-reducing disaccharide which is abundant in the cytosol of mycobacteria in free form and in the cell wall as glycolipids,[7] was used as the targeting ligand for mycobacteria. We hypothesize that trehalose-functionalized HOMSNs could effectively target mycobacteria and enhance the antibacterial activity of HOMSNs-based drug delivery system.

Trehalose-conjugated HOMSNs are prepared following the scheme shown in Figure 1 (see Supporting Information for details). OMSNs with mesoporous channels parallel to the short axis were synthesized using tetraethyl orthosilicate (TEOS) as silica precursor and cetyltrimethylammonium bromide (CTAB) as template in the mixed solvent of water and dibenzyl ether. This unique nanostructure gives OMSNs exceptional advantages in applications involving mass transfer, especially in drug delivery with regard to drug loading, entrapment efficiency, and sustained release.[4i,8] After simple hydrothermal treatment of OMSNs using ammonia, HOMSNs with hollow interior and permeable mesoporous shell were obtained. Trehalose was then conjugated on HOMSNs using our previously developed method by treating HOMSNs with PFPA-silane (*N*-(3-trimethoxysilylpropyl)-4-azido-2,3,5,6-tetrafluorobenzamide) followed by attaching trehalose by photocoupling to give HOMSNs-Tre (Figure S1).[9]

Well-ordered OMSNs with an average long-axis length of ~200 nm and short-axis width of ~100 nm were successfully synthesized (Figure 2A–C, Figure S2). After removing the CTAB template by calcination (Figure S3), the mesochannels can be clearly seen as running parallel to the short axis (Figure 2A). N_2 sorption results of OMSNs yielded a typical type IV isotherm (Figure S4A), indicating the presence of hexagonal cylindrical mesoporous channels.[10] The pore size of OMSNs was calculated to be 3.3 nm by the Barrett–Joyner–Halenda (BJH) method (Figure S4B). The Brunauer–Emmett–Teller (BET) surface area and pore volume were 1023.6 m^2/g and 0.89 cm^3/g, respectively. When OMSNs were treated with ammonia under hydrothermal conditions, HOMSNs with robust shell layer of ca. 20 nm in thickness were obtained (Figure 2D). HOMSNs retained the morphology of OMSNs without apparent changes in the particle length and width (Figure 2E–F, and S5). The structure is stable, and no apparent deformation was observed after HOMSNs were treated in PBS buffer at 37 °C for 48 h (Figure S6). The N_2 sorption results showed that HOMSNs possessed type IV isotherm with H3 hysteresis (Figure S7A), which is consistent with the

macroporous structure.[10] This was further supported by the wide pore size distribution profile of HOMSNs (Figure S7B). A sharp peak at ca. 3.7 nm suggests the presence of ordered mesoporous channels in the shell. The size of the mesopores in the shell increased from 3.3 nm to 3.7 nm after OMSNs were converted to HOMSNs, probably due to the etching effect of the ammonia hydrothermal treatment. The BET surface area and pore volume of HOMSNs changed to 479.3 m^2/g and 0.37 cm^3/g, respectively. The unique properties of HOMSNs make them an excellent candidate as drug delivery platform, including the hollow interior which can be used as a large reservoir, abundant pore channels in the shell serving as passages for mass transport, and high anisotropy for binding to target organisms.

A mechanism for the formation of HOMSNs is proposed in Figure 3. When dibenzyl ether was added to the aqueous solution of CTAB, it is expected to be preferentially dissolved in the hydrocarbon core of CTAB micelles and to swell them.[11] This hypothesis was supported by the result shown in Figure S8 that the pore size of the nanoparticles increased with increasing amount of dibenzyl ether added. TEOS induces the formation of hexagonally patterned rod-like micelles,[12] which would be shortened by the addition of dibenzyl ether (Figure S9).[4i,13] As a result, the intermediate oblate morphology was developed during the rod-to-sphere transition. The morphology and the mesopore alignment can be tuned by the amount of dibenzyl ether (Figure S8 and S9).[14] More importantly, the use of dibenzyl ether as the co-solvent gave rise to a new type of oblate mesoporous nanostructures with the pore channels running parallel to the short axis (Figure 2A). This unique morphology provides highly accessible pore channels allowing the etchant to diffuse easily into the interior of the particle. Additionally, a much milder etchant, ammonia, instead of NaOH or $NaBH_4$ can be used. As the etchant reacts with the interior silica, the produced mono-, oligo- and poly-silicate species re-deposit back to the core surface to form the shell structure.[15] Increasing the amount of CTAB resulted in the more commonly observed rod-shaped morphology with mesochannels running parallel to the long axis (Figure S10). In this case, no hollow structure could be obtained after the ammonia hypothermia treatment (Figure S11A). Spherical MSNs could be converted to hollow structures under the same conditions, however, residual silica fragments could be seen inside the core (Figure S11B). These results demonstrate that the OMSNs with the pore channels running parallel to the short axis possess a superior configuration allowing the dissolution of the core under mild conditions to give the hollow oblate nanostructures cleanly.

Trehalose was conjugated on HOMSNs using the photocoupling chemistry developed previously in our laboratory by treating HOMSNs with PFPA-silane followed by photolysis in the presence of trehalose (Figure S1, see Supporting Information for details).[9] The functionalization process was followed by FTIR (Figure S12). TGA results showed that trehalose-conjugated HOMSNs (HOMSNs-Tre) had an extra weight loss of ~8.1% (Figure S13). To compare the targeting efficiency of trehalose, D-mannose was used as a control and was conjugated to HOMSNs in the same manner as trehalose (Figure S14 and S15). The conjugation density of trehalose and mannose on HOMSNs were further measured to be about 1.8 and 3.1 molecules per nm^2, respectively, by a colorimetry assay using anthrone/sulfuric acid.[16]

Isoniazid (INH), an antimycobacterial drug that inhibits the synthesis of mycolic acid which is essential for the bacterial cell wall,[17] was chosen to encapsulate into the hollow oblate nanoparticles. The loading capacity of INH in HOMSNs, HOMSNs-Tre, and HOMSNs-Man reached 636, 563, and 594 mg per gram of nanoparticles, respectively (Figure S16). The release profile in PBS (pH 6.6, simulating the environment of 7H9 broth medium[18]) showed sustained release of INH from the hollow oblate nanostructures (Figure 4A). The amount of drug released within 48 hours was about 80%, 65%, and 70% for HOMSNs, HOMSNs-Tre, and HOMSNs-Man, respectively. The slightly lower release from HOMSNs-Tre and HOMSNs-Man compared to HOMSNs alone is probably due to the surface conjugated carbohydrates which could decrease the pore size and slow down the diffusion of the drug. *M. smegmatis* mc^2 651, an INH-resistant strain,[19] was chosen to test the antimicrobial efficacy of the resulting materials. Inhibition zone tests were conducted on INH-loaded HOMSNs (HOMSNs-INH), INH-loaded HOMSNs-Tre (HOMSNs-Tre-INH), and INH-loaded HOMSNs-Man (HOMSNs-Man-INH) samples containing the same amount of INH. In the inhibition zone test, bacteria are “immobilized” on the agar plate, therefore, the antibacterial activity of these materials relies on the amount of free INH released. As expected, the inhibition zone diameters of the materials (Figure S17) were consistent with their drug release profiles (Figure 4A).

Mycobacteria-killing assay was conducted by treating *M. smegmatis* mc^2 651 with varying concentrations of free INH, HOMSNs-INH, HOMSNs-Tre-INH, and HOMSNs-Man-INH. A dose-response relationship was observed, and the killing efficiency varied with the type of materials (Figure 4B). Free INH-treated mycobacteria were completely inhibited at a concentration of 1500 μg/mL, whereas for HOMSNs-INH, HOMSNs-Man-INH, and HOMSNs-Tre-INH, the complete inhibition of mycobacteria occurred at 1000, 1000, and 250 μg/mL, respectively. The half inhibitory concentration (IC_{50}) of mycobacteria treated by free INH drug was 1.9-, 2.5-, and 7.7- fold of HOMSNs-INH-, HOMSNs-Man-INH-, and HOMSNs-Tre-INH-treated bacteria, respectively.

Hollow oblate particles alone did not show obvious antibacterial activities (Figure S18). When INH was loaded into HOMSNs, the resulting material exhibited ~ 2 folds higher activity than free INH. This enhanced antibacterial activity is likely due to the sustained intrabacterial accumulation of INH from drug-loaded hollow oblate nanostructures, as well as the anisotropic morphology which is known to have enhanced interaction with cells.[3d,4b,4c,4e] Conjugation of mannose to HOMSNs did not result in any obvious change in the antibacterial activity of the nanoparticles. Trehalose-conjugated HOMSNs, however, showed nearly 8 folds increase in antibacterial activity. We attributed this to the ability of trehalose to specifically target mycobacteria.

To test this hypothesis, we treated mycobacteria with HOMSNs-Tre-INH and monitored the interaction of HOMSNs-Tre-INH with mycobacteria by TEM (Figure 5). Nanoparticles were attached to bacterial cell surface shortly after incubation (Figure 5B). The density of surface-adhered nanoparticles increased with time. Cell damage was observed at longer incubation time (Figure 5D–E), and eventually, cells were disintegrated (Figure 5F). In comparison, HOMSNs-INH and HOMSNs-Man-INH bound to bacteria to much less extent (Figure S19 and S20). We then counted the number of particles surrounding each bacteria

after 8 h treatment. On each bacteria cell, there were 36±18, 45±22, and 159±37 of HOMSNs-INH, HOMSNs-Man-INH, and HOMSNs-Tre-INH particles, respectively. Interestingly, the number of interacting particles correlated well with the IC_{50} results of these particles. These, together with the inhibition zone test results, strongly suggested that the enhanced antibacterial activity of HOMSNs-Tre-INH was due to the increased interactions of the particles with mycobacteria resulting from the targeting effect of trehalose.

To further test the targeting selectivity of trehalose towards mycobacteria, two strains of Gram-negative *E. Coli* bacteria (ORN178 and ORN208) and a Gram-positive *Staphylococcus epidermidis* (*S. epidermidis*) 35984 were treated with HOMSNs-Tre-INH for 8 h. Unlike the mycobacteria that were disintegrated under this condition (Figure 5F), almost no particles were observed on either *E. coli* strains or *S. epidermidis* 35984, and the cells were intact (Figures S21A–B and S22). Similarly, no obvious interactions were observed when treating *E. coli* bacteria with HOMSNs or HOMSNs-INH (Figure S21C–D). These results demonstrate the specific targeting ability of trehalose to mycobacteria.

In summary, we developed a straightforward and effective method to synthesize trehalose-functionalized hollow oblate mesoporous silica nanoparticles to target mycobacteria. The use of dibenzyl ether as the co-solvent gave OMSNs having mesochannels running parallel to the short axis. This unique configuration creates high density of pore channels which allowed the conversion of OMSNs to HOMSNs by a simple ammonia hydrothermal treatment. These hollow oblate mesoporous nanoparticles showed high drug loading capacities and sustained drug release profiles. We have furthermore demonstrated that trehalose can be used as an effective targeting agent for mycobacteria, and trehalose-conjugated HOMSNs greatly enhanced the antibacterial activity of INH. The method developed here for the synthesis of hollow mesoporous silica nanoparticle-based nanoantibiotics is versatile, and is applicable to different targeting ligands and theranostic agents. The unique characteristics of these nanostructures such the anisotropic morphology, hollow interior and ample pore channels in the shell, could also find applications in other areas such as catalysis, adsorption, sensing, and separation.

Supplementary Material

Refer to Web version on PubMed Central for supplementary material.

Acknowledgments

We thank Professor William R. Jacobs of Albert Einstein College of Medicine for his kind donation of *M. smegmatis* strain mc^2 651. This work was supported by National Institutes of Health (R01GM080295, 1R21AI109896-01), and a startup grant from University of Massachusetts Lowell.

References

1. a) Sherrard LJ, Tunney MM, Elborn JS. Lancet. 2014; 384:703. [PubMed: 25152272] b) Brooks BD, Brooks AE. Adv Drug Deliv Rev. 2014; 78:14. [PubMed: 25450262] c) Piddock LJ. Microbiology. 2014; 160:2366. [PubMed: 25122880]
2. a) Stein A, Melde BJ, Schroden RC. Adv Mater. 2000; 12:1403.b) Torney F, Trewyn BG, Lin VSY, Wang K. Nat Nanotechnol. 2007; 2:295. [PubMed: 18654287] c) Slowing II, Trewyn BG, Giri S,

Lin VSY. Adv Funct Mater. 2007; 17:1225.d) Trewyn BG, Giri S, Slowing II, Lin VSY. Chem Commun. 2007; 43:3236.e) Hudson S, Cooney J, Magner E. Angew Chem. 2008; 120:8710.Angew Chem Int Ed. 2008; 47:8582.f) Thanh NTK, Green LaW. Nano Today. 2010; 5:213.g) Manzano M, Vallet-Regí M. J Mater Chem. 2010; 20:5593.h) Vivero-Escoto JL, Slowing II, Trewyn BG, Lin VSY. Small. 2010; 6:1952. [PubMed: 20690133] i) Barreto JA, O'Malley W, Kubeil M, Graham B, Stephan H, Spiccia L. Adv Mater. 2011; 23:H18. [PubMed: 21433100] j) Dai CL, Guo H, Lu JX, Shi JL, Wei J, Liu CS. Biomaterials. 2011; 32:8506. [PubMed: 21864896]

3. a) Liong M, France B, Bradley KA, Zink JI. Adv Mater. 2009; 21:1684.b) Zhu M, Wang HX, Liu JY, He HL, Hua XG, He QJ, Zhang LX, Ye XJ, Shi JL. Biomaterials. 2011; 32:1986. [PubMed: 21163519] c) Clemens DL, Lee BY, Xue M, Thomas CR, Meng H, Ferris D, Nel AE, Zink JI, Horwitz MA. Antimicrob Agents Chemother. 2012; 56:2535. [PubMed: 22354311] d) Hao NJ, Jayawardana KW, Chen X, Yan M. ACS Appl Mater Interfaces. 2015; 7:1040. [PubMed: 25562524]
4. a) Champion JA, Mitragotri S. Proc Natl Acad Sci USA. 2006; 103:4930. [PubMed: 16549762] b) Champion, Ja; Katare, YK.; Mitragotri, S. J Control Release. 2007; 121:3. [PubMed: 17544538] c) Geng Y, Dalhaimer P, Cai SS, Tsai R, Tewari M, Minko T, Discher DE. Nat Nanotechnol. 2007; 2:249. [PubMed: 18654271] d) Huang XL, Teng X, Chen D, Tang FQ, He JQ. Biomaterials. 2010; 31:438. [PubMed: 19800115] e) Vácha R, Martinez-Veracoechea FJ, Frenkel D. Nano Lett. 2011; 11:5391. [PubMed: 22047641] f) Shah S, Liu YL, Hu W, Gao JM. J Nanosci Nanotechnol. 2011; 11:919. [PubMed: 21399713] g) Hao NJ, Li LL, Zhang Q, Huang XL, Meng XW, Zhang YQ, Chen D, Tang FQ. Microporous Mesoporous Mater. 2012; 162:14.h) Hao NJ, Li LF, Tang FQ. J Biomed Nanotechnol. 2014; 10:2508. [PubMed: 25992407] i) Hao NJ, Li LF, Tang FQ. J Mater Chem A. 2014; 2:11565.j) Hao NJ, Yang HH, Li LF, Li LL, Tang FQ. New J Chem. 2014; 38:4258.
5. a) (David) Lou XW, Archer LA, Yang ZC. Adv Mater. 2008; 20:3987.b) Liu J, Qiao SZ, Chen JS, Lou XW, Xing XR, Lu GQ. Chem Commun. 2011; 47:12578.
6. Gatfield J, Pieters J. Science. 2000; 288:1647. [PubMed: 10834844]
7. a) Indrigo J, Hunter RL, Actor JK. Microbiology. 2003; 149:2049. [PubMed: 12904545] b) Pan YT, Koroth Edavana V, Jourdian WJ, Edmondson R, Carroll JD, Pastuszak I, Elbein AD. Eur J Biochem. 2004; 271:4259. [PubMed: 15511231] c) Woodruff PJ, Carlson BL, Siridechadilok B, Pratt MR, Senaratne RH, Mougous JD, Riley LW, Williams SJ, Bertozzi CR. J Biol Chem. 2004; 279:28835. [PubMed: 15102847] d) Geisel RE, Sakamoto K, Russell DG, Rhoades ER. J Immunol. 2005; 174:5007. [PubMed: 15814731]
8. Zhang H, Sun JM, Ma D, Bao XH, Klein-Hoffmann A, Weinberg G, Su DS, Schlögl R. J Am Chem Soc. 2004; 126:7440. [PubMed: 15198581]
9. a) Yan M, Harnish B. Adv Mater. 2003; 15:244.b) Yan M, Ren J. Chem Mater. 2004; 16:1627.c) Liu L, Yan M. Angew Chem. 2006; 118:6353.Angew Chem Int Ed. 2006; 45:6207.d) Liu LH, Yan M. Nano Lett. 2009; 9:3375. [PubMed: 19670850] e) Liu LH, Yan M. Acc Chem Res. 2010; 43:1434. [PubMed: 20690606] f) Park J, Yan M. Acc Chem Res. 2013; 46:181. [PubMed: 23116448] g) Chen X, Ramström O, Yan M. Nano Res. 2014; 7:1381. [PubMed: 26500721]
10. Sing KSW, Everett DH, Haul RAW, Moscou L, Pierotti RA, Rouquerol J, Siemieniewska T. Pure Appl Chem. 1985; 57:603.
11. a) Ottaviani MF, Moscatelli A, Desplantier-Giscard D, Di Renzo F, Kooyman PJ, Alonso B, Galarneau A. J Phys Chem B. 2004; 108:12123.b) Peng J, Liu J, Liu J, Yang Y, Li C, Yang QH. J Mater Chem A. 2014; 2:8118.
12. a) Kresge CT, Leonowicz ME, Roth WJ, Vartuli JC, Beck JS. Nature. 1992; 359:710.b) Sayari A, Han BH, Yang Y. J Am Chem Soc. 2004; 126:14348. [PubMed: 15521742]
13. Shen SD, Gu T, Den Mao D, Xiao XZ, Yuan P, Yu MH, Xia LY, Ji Q, Meng L, Song W, Yu CZ, Lu GZ. Chem Mater. 2012; 24:230.
14. Yu CZ, Fan J, Tian BZ, Zhao DY. Chem Mater. 2004; 16:889.
15. a) Lin HP, Mou CY, Liu SB. Adv Mater. 2000; 12:103.b) Zhang TR, Ge JP, Hu YX, Zhang Q, Aloni S, Yin YD. Angew Chem. 2008; 120:5890.Angew Chem Int Ed. 2008; 47:5806.c) Zhang HN, Zhou Y, Li YR, Bandosz TJ, Akins DL. J Colloid Interf Sci. 2012; 375:106.
16. a) Wang X, Ramström O, Yan M. Chem Commun. 2011; 47:4261.b) Wang X, Matei E, Gronenborn A, Ramström O, Yan M. Anal Chem. 2012; 84:4248. [PubMed: 22548468] c) Jayawardena HSN, Jayawardana KW, Chen X, Yan M. Chem Commun. 2013; 49:3034.
17. Takayama K, Davidson LA. Trends Biochem Sci. 1979; 4:280.

18. Carlson LDC, Wallis CK, Coyle MB, Carlson LADC. J Clin Microbiol. 1998; 36:748. [PubMed: 9508306]

19. a) Fu LM, Shinnick TM. Tuberculosis. 2007; 87:63. [PubMed: 16890025] b) Siu GK, Yam WC, Zhang Y, Kao RY. Antimicrob Agents Chemother. 2014; 58:6093. [PubMed: 25092698]

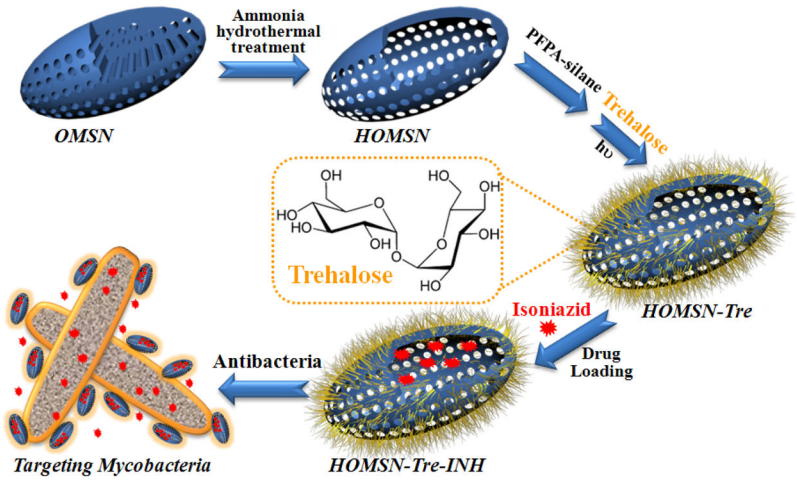

Figure 1.
Fabrication of trehalose-conjugated HOMSN nanoantibiotic system.

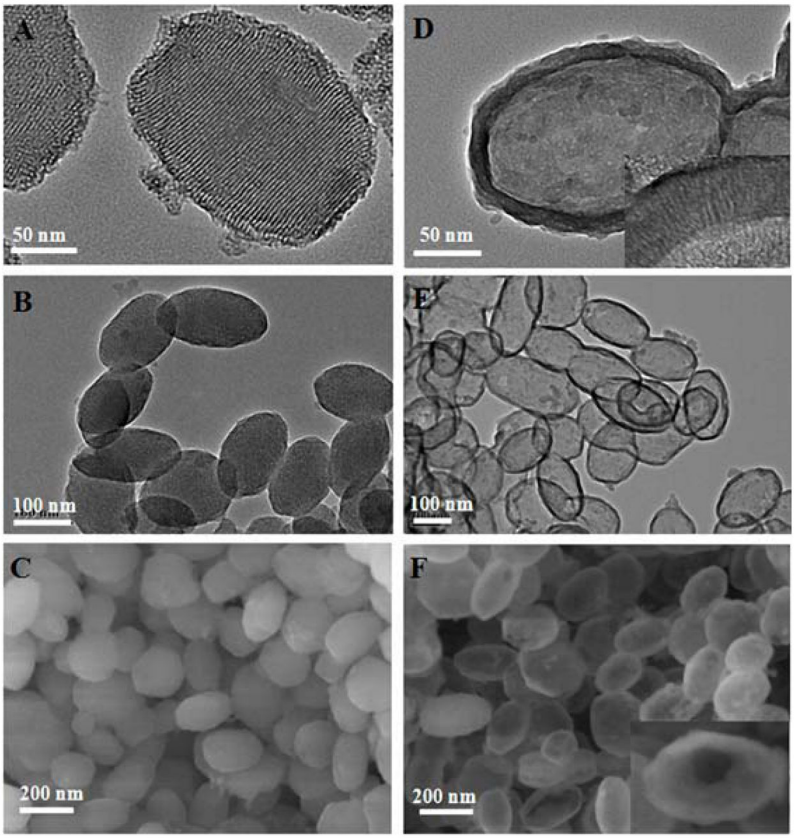

Figure 2.

(A), (B) TEM images of OMSNs at different magnifications. (C) SEM image of OMSNs. (D)–(E) TEM images of HOMSNs at different magnifications. (F) SEM image of HOMSNs. The inset in (D) shows porous nanochannels in the shell, and the inset in (F) shows the hollow interior of a HOMSN.

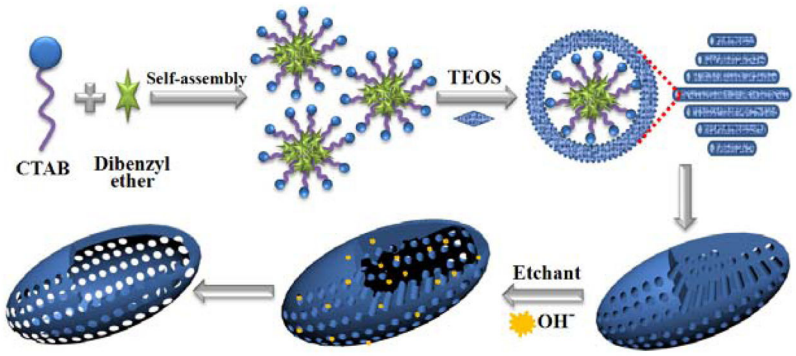

Figure 3.
The proposed mechanism for the formation of HOMSNs.

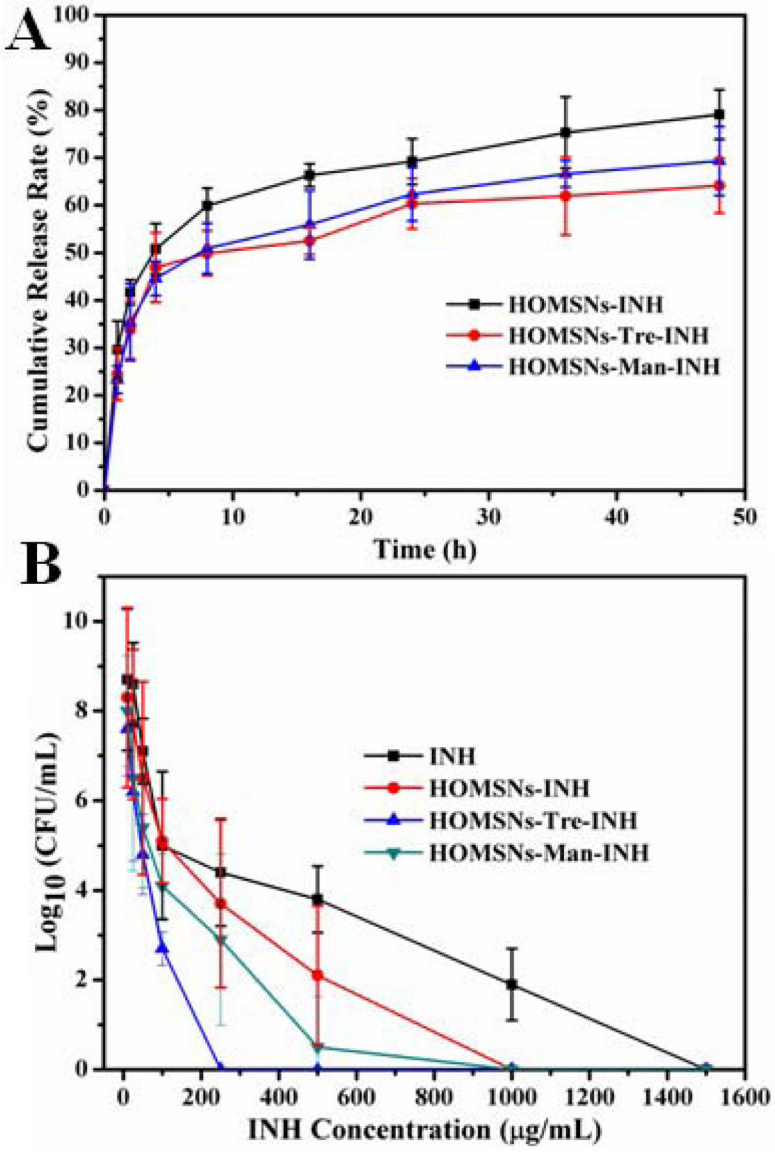

Figure 4.

(A) Release profile of INH from drug-loaded particles (HOMSNs-INH, HOMSNs-Tre-INH, and HOMSNs-Man-INH) within the first 48 hours in PBS buffer (pH 6.6). (B) Antibacterial efficacy of free INH and INH-loaded particle samples (at concentration of INH from 10 to 1500 μg/mL) on *M. smegmatis* strain mc^2 651 for 48 h. The IC_{50} values were 729, 376, 95, and 293 μg/mL for INH, HOMSNs-INH, HOMSNs-Tre-INH, and HOMSNs-Man-INH, respectively.

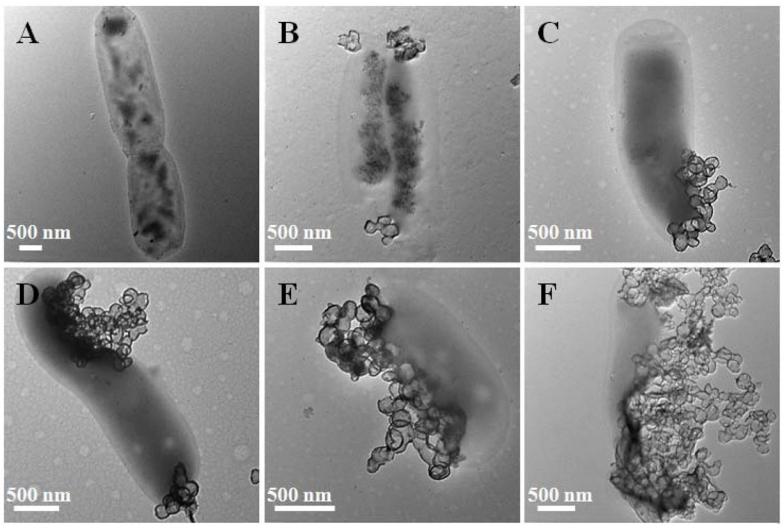

Figure 5.
TEM images of mycobacteria treated with HOMSNs-Tre-INH for 0 h (A), 0.5 h (B), 1 h (C), 2 h (D), 4 h (E), and 8 h (F).